High-Affinity Triple Helix Formation by Synthetic Oligonucleotides at a Site within a Selectable Mammalian Gene†

Karen M. Vasquez,‡ Theodore G. Wensel,‡ Michael E. Hogan,§ and John H. Wilson*,‡

Verna and Marrs McLean Department of Biochemistry and Department of Molecular Physiology and Biophysics, Baylor College of Medicine, One Baylor Plaza, Houston, Texas 77030

Received January 30, 1995; Revised Manuscript Received March 24, 1995⊗

ABSTRACT: Specific recognition of duplex DNA by a single-stranded oligonucleotide via the formation of triplex DNA is a rational approach for targeting specific regions of a genome. By screening a number of potential target sites for triple helix formation within mammalian genes that allow genetic selection in cell culture, we have identified a site within intron 1 of the hamster adenine phosphoribosyltransferase (APRT) gene that specifically binds a triplex-forming oligodeoxyribonucleotide (TFO) with high affinity. Under optimal conditions for triplex formation, the equilibrium dissociation constant is in the nanomolar range ($K_d = 7 \times 10^{-10}$ M). This high-affinity binding is very specific, as a 10^5-fold excess of genomic DNA reduced triplex formation less than 10-fold, and within a 6928-bp plasmid bearing the APRT gene, only restriction fragments containing the intron 1 site were found to bind the TFO. Results of DNase I protection assays were consistent with the TFO binding in an antiparallel orientation via reverse Hoogsteen hydrogen bonds in the major groove of the duplex. We have examined the kinetics of triplex formation as well as the effects of ionic composition and chemical modifications of the TFO on triplex formation. While divalent cations were not required for triplex formation, Mg^{2+} stabilized the triplex apparently through inhibition of TFO dissociation, with a mean bound lifetime of >17 h for the triplex at Mg^{2+} concentrations above 5 mM. Monovalent cations had little or no effect on triplex formation at low concentrations (10 mM) but had a negative effect at higher concentrations, with inhibition of triplex formation in the order $K^+ \gg Li^+ \geq Na^+$. Binding of a 6-thioguanosine (6-TG) modified TFO was much less sensitive to K^+ than binding of the unmodified TFO, consistent with 6-TG inhibition of G-quartet formation, a likely K^+-dependent competing reaction. Finally, the TFO containing thymines at positions interacting with cytosine bases in the duplex formed triplex with an affinity similar to those of TFOs containing either an imidazole derivative or 5-fluorouracil in place of thymine.

Targeting of triplex-forming oligonucleotides to specific sites on chromosomes represents a promising approach to gene manipulation in living cells. In order to achieve specific binding in the presence of high levels of nontarget DNA within the eukaryotic nucleus, triple helix formation must occur with high affinity and specificity. Consequently, considerable effort has been expended to optimize the design of triplex-forming oligonucleotides (TFOs)[1] for biomedical applications and to characterize the effects of ionic composition (Rougee et al., 1992; Singleton & Dervan, 1993; Thomas & Thomas, 1993; Cheng & Van Dyke, 1993; Bond et al., 1994), chemical modifications (Maher et al., 1989; Milligan et al., 1993; Stilz & Dervan, 1993; Durland et al., 1994), pH (Krawczyk et al., 1992; Singleton & Dervan, 1992; Jetter & Hobbs, 1993), and temperature (Hanvey et al., 1991; Pilch et al., 1991) on triplex formation.

Since the original description of triple helical nucleic acid structures (Felsenfeld et al., 1957), a number of different motifs have been studied. These include homopurine, homopyrimidine, and mixed purine/pyrimidine third strands binding in the major groove of the underlying DNA duplex through either Hoogsteen or reverse Hoogsteen hydrogen bonding patterns (Thuong & Helene, 1993). Purine-rich TFOs, which can hydrogen bond to the purine-rich strand in target duplexes in an antiparallel orientation (Cooney et al., 1988; Hogan et al., 1989; Beal & Dervan, 1991), are particularly advantageous for applications in living cells because, unlike pyrimidine-rich TFOs, they can form stable triplexes at neutral pH (Rajagopal & Feigon, 1989) without base modification. A number of reports have been published on the kinetics and thermodynamics of parallel triplexes formed by pyrimidine-rich TFOs (Maher et al., 1990; Rougee et al., 1992; Shindo et al., 1993; Singleton & Dervan, 1993) and on the effects of cations (Rougee et al., 1992; Singleton & Dervan, 1993; Thomas & Thomas, 1993; Bond et al., 1994) and chemical modifications of bases (Maher et al., 1989; Povsic & Dervan, 1989; Krawczyk et al., 1992) on their triplex formation. In contrast, there have been few studies of antiparallel triplexes formed by purine-rich TFOs (Moser & Dervan, 1987; Cheng & Van Dyke, 1993; Milligan et al., 1993; Durland et al., 1991).

TFOs have been used to inhibit the binding of proteins to DNA (Maher et al., 1989; Grigoriev et al., 1992; Mayfield et al., 1994), to inhibit gene expression (Cooney et al., 1988; Postel et al., 1991; Duval-Valentin et al., 1992; McShan et

† This work was funded by grants from the NIH to J.H.W. (GM38219 and DK42678) and M.E.H. (A132804), a grant from the Welch Foundation to T.G.W. (Q1179), and Triplex Pharmaceutical Corporation.

‡ Verna and Marrs McLean Department of Biochemistry.

§ Department of Molecular Physiology and Biophysics.

⊗ Abstract published in *Advance ACS Abstracts,* May 1, 1995.

[1] Abbreviations: APRT, adenine phosphoribosyltransferase; CHO, Chinese hamster ovary; HPRT, hypoxanthine phoshphoribosyltransferase; TFO, triplex-forming oligodeoxyribonucleotide; 5FU, 2′-deoxy-5-fluorouracil; 6-TG, 2′-deoxy-6-thioguanosine.

0006-2960/95/0434-7243$09.00/0

al., 1992; Grigoriev et al., 1993; Ing et al., 1993), to direct targeted mutagenesis (Havre et al., 1993; Havre & Glazer, 1993), to purify specific DNA sequences by triplex affinity capture (Ito et al., 1992), and to induce site-specific DNA damage (Moser & Dervan, 1987; Pei et al., 1990; Perrouault et al., 1990; Strobel & Dervan, 1991; Le Doan et al., 1991). A particularly promising application of triplex technology is its use to study and manipulate genetic recombination in mammalian cells. Targeted homologous recombination has proven valuable in studies of gene function and in biotechnology (Rothstein, 1983; Botstein & Fink, 1988; Mansour et al., 1988) and has been proposed as an approach to gene therapy (Capecchi, 1991). Of the few mammalian genes whose function can be conveniently studied by both positive and negative selection in cell culture, one of the most useful, and best characterized, is the hamster APRT gene. Cell lines that bear a variety of mutant APRT genes have been created, and well-defined selection schemes allow sensitive detection of rare recombinogenic and mutagenic events (Adair et al., 1989, 1990; Pennington & Wilson, 1991).

In order to exploit the potential of targeted triplex formation in the APRT system, we have searched for sites within the hamster APRT gene that bind with high affinity to purine-rich TFOs. We describe here the identification of one such high-affinity site within the APRT gene and its characterization with respect to equilibrium and kinetic binding properties, binding specificity, and effects of ionic composition. In addition, we describe effects of chemical modifications of the TFO on triplex formation.

EXPERIMENTAL PROCEDURES

Oligonucleotide Synthesis and Purification. The sequences and modifications of the oligodeoxyribonucleotides used are shown in Table 1. They were synthesized on an automated MilliGen 8700 DNA synthesizer (Millipore Corp., Milford, MA) using standard solid-phase chemistry. β-Cyanoethyl phosphoramidites were purchased from Millipore, and Amino-Modifier controlled pore glass and 2′-deoxy-5-fluorouracil were purchased from Glen Research Corporation (Sterling, VA). Dimethoxytrityl phoshphoramidites of 2′-deoxy-6-thioguanosine and imidazole-2′-deoxyribonucleoside were obtained from Triplex Pharmaceutical Corporation (Rao et al., 1992). The phosphoramidite derivative of 2′-deoxy-5-fluorouracil was purchased from Glen Research Corporation. Oligos were deprotected by incubating in a solution of 0.1 N NaOH at 55 °C for at least 24 h, and then purified by reverse-phase HPLC using a C18 (Waters) column and a gradient of acetonitrile (0−50%) in 0.1 M triethylammonium acetate, pH 7.3. Aqueous acetic acid, 80%, was used for detritylation. Oligos were suspended in 100 mM NaCl, desalted on a NAP-5 column (Pharmacia LKB Biotechnology, Uppsala, Sweden) equilibrated with Milli-Q water, and dried. Oligonucleotides were then gel purified by denaturing PAGE (15% acrylamide). Bands were visualized by UV shadowing, cut from the gel, and eluted by soaking in H_2O at 55 °C for 12 h. Oligos were then concentrated by centrifugation in a Centricon (Amicon Div., W. R. Grace & Co.-Conn., Beverly, MA) filter unit. The concentration of DNA was determined by UV absorbance. Oligonucleotides were 5′-end labeled using T4 polynucleotide kinase (Boehringer Mannheim, Indianapolis, IN) and [γ-^{32}P]ATP (6000 Ci/mmol) (New England Nuclear Research Products, Boston, MA).

Preparation of Plasmid pGS37 Fragments for Specificity Tests. Plasmid pGS37 (provided by Dr. Geoff Sargent) was constructed by subcloning the hamster APRT gene as an *Eco*RI fragment into pBluescript II SK (Stratagene, La Jolla, CA), $CsCl_2$ purified and stored at −20 °C at a concentration of 1 mg/mL. For DNase I footprinting, a 196-bp *Eco*RV to *Pvu*II fragment containing the hamster APRT gene was isolated from plasmid pGS37. The fragment was [γ-^{32}P]-ATP labeled on the 5′ end of the purine-rich strand of the duplex using phosphatase and then T4 polynucleotide kinase at the *Eco*RV site. The fragment was gel purified on a native 5% polyacrylamide gel, electroeluted in TBE (89 mM Tris, 89 mM boric acid, and 2 mM EDTA) buffer, and concentrated by centrifugation in a Centricon (Amicon) filter unit.

Restriction Fragment Binding Analysis. Digestion reactions with endonuclease restriction enzymes *Nhe*I and *Sty*I, (New England Biolabs Inc., Beverly, MA) were performed at 37 °C for 12 h using 5 μg of plasmid DNA in a total volume of 30 μL. DNA was then EtOH precipitated, resuspended, and incubated at 37 °C in triplex binding buffer (10 mM Tris-HCl, pH 7.6, 10 mM $MgCl_2$, 1 mM spermine, and 10% sucrose) with an equimolar concentration of 5′-^{32}P-labeled TFO. Samples were subjected to electrophoresis through a 1% agarose gel containing 5 mM $MgCl_2$, 89 mM Tris, and 89 mM boric acid. Restriction fragments were visualized by EtBr staining, and triplexes were detected by autoradiography.

DNase I Protection Analysis. The 5′-end-labeled 196-bp *Eco*RV to *Pvu*II plasmid fragment containing the APRT intron 1 target site or a 5′-end-labeled 38-bp synthetic duplex was incubated with 1×10^{-6} M TFO in triplex binding buffer at 37 °C in a final volume of 10 μL for 15 h to allow complex formation to reach equilibrium. DNase I at 0.125 units/mL was then added, and samples were further incubated at 37 °C for 15 min. Ninety microliters of a solution containing 500 mM Tris-HCl, pH 7.6, 20 mM EDTA, and 90 μg/mL calf thymus DNA was subsequently added to stop the reaction. Samples were subjected to electrophoresis on 15% polyacrylamide denaturing gels, dried, and autoradiographed.

Band Shift Analysis. Oligonucleotides (38 bp) corresponding to the APRT sequence around the intron 1 site were annealed in a 1:1 molar ratio to form a target duplex. Duplex was 5′-end-labeled using T4 polynucleotide kinase and [γ-^{32}P]ATP, gel purified, and incubated for the indicated times with increasing concentrations of TFO in buffer containing 10 mM Tris-HCl, pH 7.6, 1 mM spermine, 10% sucrose, and appropriate concentrations of salts to give the desired final concentrations of the cations as indicated in the figure captions. Gel mobility shift assays were performed by electrophoresis through a native 12% polyacrylamide gel containing 89 mM Tris, 89 mM boric acid, pH 8.0, and 10 mM $MgCl_2$ (unless otherwise noted). Gels were run for 3−4 h at 60 V at 22 °C, dried, and autoradiographed. For quantitation, radioactivity in each band was measured using a Betagen Beta Scope 603 blot analyzer. Apparent dissociation constants determined following 15-h incubations are indicated as K_{app}.

RESULTS

Screening of Potential Triplex-Forming Sites in hamster APRT and Human HPRT Genes. A computer search was conducted to identify potential triplex-forming target sites in both the hamster APRT gene and the human hypoxanthine

Table 1. Potential Triplex Forming Sites Screened[a]		
TARGET SITE: APRT INTRON 1		K_{app} (M)[b]
5'-GCTGGTGGCCGGGGAAAGGGGGGCGGAGACCCCACAAG-3'		
3'-GGGGTTTGGGGGGTGGTGT-5'	TFO1	2×10^{-9}
3'-G**6**GGTTTG**6**GG**6**G**I**GGTGT-5'	TFO2	5×10^{-8}
3'-GGGGTTTGGGGGG**F**GGTGT-5'	TFO3	$\sim 10^{-9}$
3'-GGGG**FFF**GGGGGG**F**GG**F**G**F**-5	TFO4	$\sim 10^{-9}$
3'-GGGGTTTGGGGGG**I**GGTGT-5'	TFO5	$\sim 10^{-9}$
3'-GG**6**GTTTG**6**GG**6**G**I**GGTGT-5'	TFO6	5×10^{-8}
3'-GGGGTTTGGGGGGTGGTGT**KKK**-5'	TFO7	10^{-8}
3'-**KKK**-GGGGTTTGGGGGGTGGTGT**KKK**-5'	TFO8	10^{-8}
3'-**CHOL**-GGGGTTTGGGGGGTGGTGT-5'	TFO9	$\sim 10^{-9}$
3'-GGGGTTTGGGGGG**N**GGTGT-5'	TFO10	10^{-8}
3'-GGGG**NNN**GGGGGG**N**GG**N**G**N**-5'	TFO11	10^{-8}
5'-GGGGTTTGGGGGGTGGTGT-3'	TFO12	$> 10^{-6}$
TARGET SITE: APRT EXON 2		
5'-TGGAAGCTCGGAAGGAGGCGGGGTCCTTCAGGAGGGGCGAGATATCCCTG-3'		
3'-GGTTGGTGGTGGGG-5'	TFO13	$> 10^{-6}$
3'-GGTTGGTGG**I**GGGG-5'	TFO14	$> 10^{-6}$
3'-TGGTGGGGTGTGT-5'	TFO15	$> 10^{-6}$
3'-TGGTGGGG**I**GTGT-5'	TFO16	$> 10^{-6}$
3'-GGTTGGTGGTGGGG-**LLLL**-TGGTGGGGTGTGT-5'	TFO17	$> 10^{-6}$
3'-GGTTGGTGG**F**GGGG-**LLLL**-TGGTGGGG**F**GTGT-5'	TFO18	$> 10^{-6}$
3'-GGTTGGTGGTGGGG-**LLLLL**TGGTGGGGTGTGT-5'	TFO19	$> 10^{-6}$
3'-GGTTGGTGGTGGGG-**LLKLL**TGGTGGGGTGTGT-5'	TFO20	$> 10^{-6}$
3'-GGTTGGTGGTGGGG--$\mathbf{K_7}$--TGGTGGGGTGTGT-5'	TFO21	$> 10^{-6}$
TARGET SITE: APRT EXON 5		
5'-ACTTAAGGGCAGAGAGAAGCTAGGATCAGTACCATTCTTCTCTCTCCTGCAATAT-3'		
3'-TTGGGTTGTGTGTTGTTTGGT-5'	TFO22	$> 10^{-6}$
5'-TTGGGTTGTGTGTTGTTTGGT-3'	TFO23	$> 10^{-6}$
3'-TTGGG**F**TGTGTGTTG**FF**TGGT-5'	TFO24	$> 10^{-6}$
3'-**FF**GGG**FF**G**F**G**F**G**FF**G**FFF**GG**F**-5'	TFO25	$> 10^{-6}$
TARGET SITE: HPRT EXON 3		
5'-TCTTGCTCGAGATGTGATGAAGGAGATGGGAGGCCATCACATTGTAGC-3'		
3'-GTTGTTGGTGTTGGGTGG-5'	TFO26	$> 10^{-6}$
5'-GTTGTTGGTGTTGGGTGG-3'	TFO27	$> 10^{-6}$
TARGET SITE: HPRT INTRON 4		
5'-CAAGACATTCTAGAAGAAAAAGAGAAATGAAAATCAGTACAATGAATA-3'		
3'-TGTTGTTTTTGTGTTTTGTTTT-5'	TFO28	$> 10^{-6}$
5'-TGTTGTTTTTGTGTTTTGTTTT-3'	TFO29	$> 10^{-6}$

[a] The purine-rich strand for each of the five target duplexes tested is shown; the site at which triplex is expected to form is underlined. TFOs that were tested are aligned under the target site. Modifications were as follows: Each TFO except those with 3′-cholesterol had a 3-propanolamine modification. Base modifications are indicated in boldface type: **6** = 6-thioguanosine; **F** = 5 fluorouracil; **I** = base replacement with imidazole; **K** = 5 rotatable bond linker as described (Kessler et al., 1993); **CHOL** = cholesterol derivative (Vu et al., 1993); **N** = amino modifier C6 dT (Glen Research); **L** = 11 rotatable bond linker (Kessler et al., 1993). [b] Triplex formation was assessed by band shift analysis after incubation under standard conditions for 15 h.

phosphoribosyltransferase (HPRT) gene using the sequences in the Genbank database. Sequences were scanned for those containing a minimum of 80% purines over a 15-bp stretch, and five potential sites were identified. These five potential triplex-forming target duplexes and corresponding TFOs designed to bind in either parallel or antiparallel orientations were synthesized and assayed for triplex formation by gel mobility shift assay (Table 1). In the initial screen, only one TFO (TFO1) was found to bind its target duplex with high affinity (*i.e.*, $K_d < 10^{-7}$ M); it binds with a $K_d < 10^{-9}$ M.

Effects of TFO Modifications on Triplex Formation. In addition to the 3′-propanolamine group incorporated into TFO1 and most of the others tested, several other modifications were introduced in attempts either to enhance binding affinity (for example, use of linkers to join purine stretches interrupted by a pyrimidine tract) or to introduce groups that increase the utility of TFOs for gene targeting in cells (for

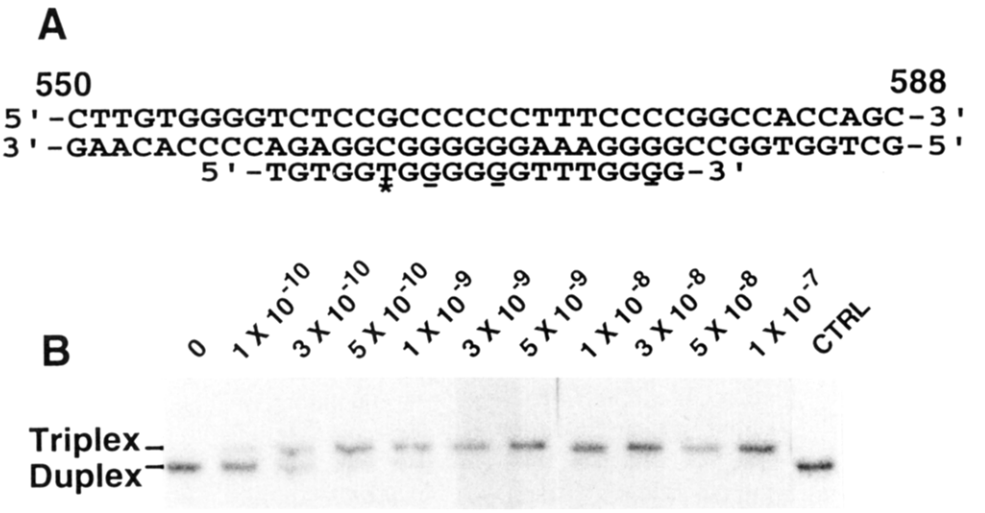

FIGURE 1: Triplex formation at the APRT intron 1 site. (A) Nucleotide sequences of synthetic APRT intron 1 target site duplex and TFO1 with the positions of base modifications indicated with an asterisk for the CG inversion site and underlined where Gs have been replaced with 6-TG in TFO2. Both TFOs were modified with a 3′-propanolamine (3′-$OPO_2OCH_2CHOHCH_2NH_3^+$) group. The expected location and orientation of TFO binding is depicted. (B) Band shift analysis of triplex formation. End-labeled target duplex was incubated with increasing concentrations of TFO in standard triplex binding buffer as indicated and subjected to PAGE. The control lane (CTRL) shows the result obtained with 10^{-6} M control having a base composition identical to that of TFO1, but a scrambled sequence.

example, use of 3′-cholesterol to enhance cellular uptake, or introduction of readily derivatized primary amines). None of these modifications resulted in significant enhancement of triplex formation, and regardless of the modification tried, only TFOs closely related to TFO1 showed high-affinity triplex formation (Table 1). However, a number of modifications were compatible with high-affinity triplex formation at the APRT intron 1 site. Replacement of thymine at various positions with imidazole or 5-fluorouracil neither enhanced nor substantially reduced triplex formation. Substitution with a thymine derivative containing a primary amine at the 5 position, or inclusion of linkers containing primary amines at either the 5′ or the 3′ end, or both, decreased binding, but the modified TFOs still bound with fairly high affinity. The largest effect of a substitution was observed when 6-thioguanosine (6-TG) was substituted for several Gs in TFO1. TFO2 and TFO6, which also had imidazole in place of T at position 564, showed an approximately 25-fold reduction in efficiency of triplex formation as compared to either TFO1 or the imidazole-bearing TFO5; as discussed below, these 6-TG-modified TFOs also showed lower sensitivity to physiological concentrations of K^+.

High-Affinity Triplex Formation at a Site within APRT Intron 1. The target site for TFO1 within the 38-mer duplex corresponds to nucleotides 559−577 within intron 1 of the APRT gene (Figure 1A). TFO1 was designed to bind in an antiparallel fashion forming G:G-C and T:A-T triplets by hydrogen bonding trhough the major groove in a reverse Hoogsteen motif. Band shift assays (Figure 1B) were used to measure the affinity of TFO1 for the intron 1 site, using Mg^{2+}-containing polyacrylamide gels which maintained triplex DNA during electrophoresis (Cooney et al., 1988). The result from a typical experiment is shown in Figure 1B. On the basis of a large number of such experiments, under our standard conditions (10 mM Tris-HCl, pH 7.6, 10 mM $MgCl_2$, 1 mM spermine, and 10% sucrose) the K_d for triplex formation between TFO1 and the intron 1 target site was $<10^{-9}$ M.

Specificity of TFO1 Binding to the Intron 1 Site. The specificity of TFO1 binding was assessed by DNase I protection analysis on the 196-bp plasmid fragment containing the intron 1 site target duplex. The protection of bases 559−577 from DNase I cleavage shows that TFO1 binds in the predicted location (Figure 2A). To further localize the site within the 38-mer target site, a DNase I protection assay was performed using the synthetic duplex (Figure 2B). Base

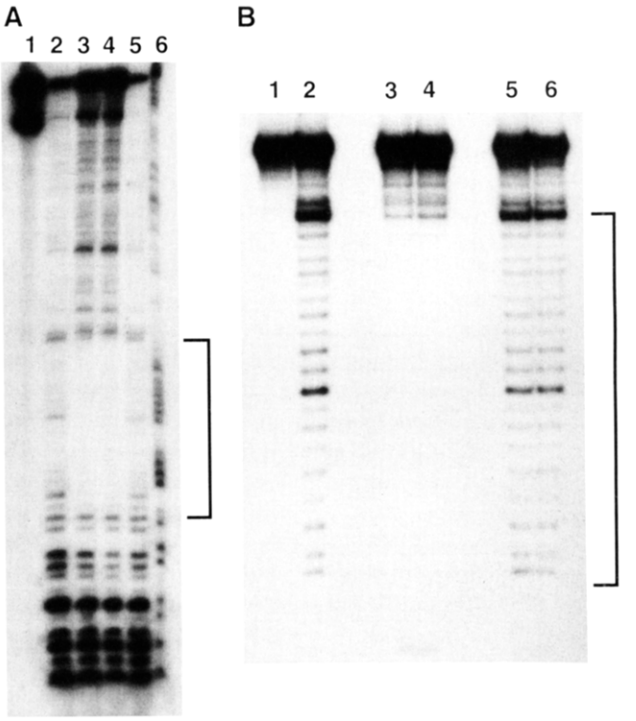

FIGURE 2: DNase I protection analysis of triplex formation. (A) A 196-bp plasmid fragment containing the APRT intron 1 site was 5′-end-labeled on the purine-rich strand of the target duplex. Lane 1, duplex without DNase I; lane 2, duplex with DNase I; lane 3, duplex + TFO1; lane 4, duplex + TFO2; lane 5, duplex + CTRL TFO; lane 6, duplex treated with DMS and piperidine to indicate location of Gs in the sequence. The expected region of triplex formation is indicated by the bracket. (B) The DNase I protection assay was performed in the same manner, with the only difference being the size of the target duplex. Here, the 38-mer synthetic target site was assayed for protection from cleavage afforded by the TFO.

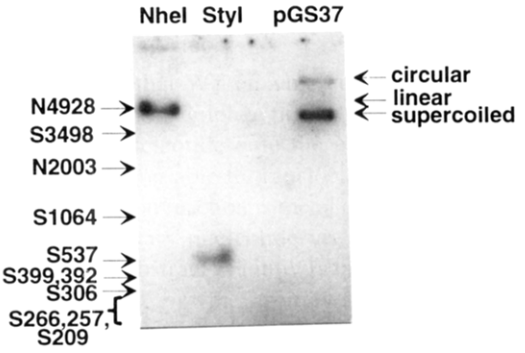

FIGURE 3: Specificity of TFO binding as shown by binding of radiolabeled TFO1 to undigested plasmid (pGS37) or to fragments generated by restriction endonucleases (*Nhe*I and *Sty*I). [^{32}P]TFO1 was incubated for 15 h with the products of extensive digestion before electrophoretic separation on a 1% agarose gel containing 5 mM $MgCl_2$, ethidium stained and autoradiographed. The arrows depict bands of the indicated molecular weights, visualized by ethidium fluorescence, and the bracket indicates the expected mobility of smaller fragments. N, fragments generated from *Nhe*I digestion; S, *Sty*I digestion. Fragments N4928 and S537 are the only fragments containing the intron 1 target site.

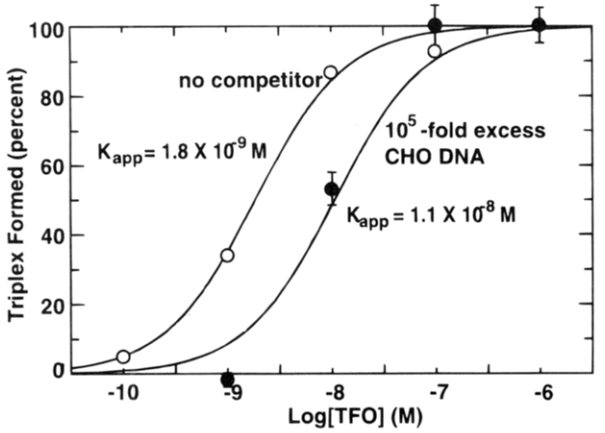

FIGURE 4: Effects of competing nontarget DNA. Genomic DNA was isolated from a Chinese hamster ovary cell line (U1S36), sonicated, and incubated with increasing concentrations of TFO at a 10^5-fold molar excess to target duplex (bp:bp) in the sample. Band shift analysis was performed as described in Experimental Procedures. Theoretical curves were fit to the data points using nonlinear least squares analysis.

pairs 559−577 were protected, confirming precise binding to the expected sequences.

The ability of TFO1 to bind to its intended target in the presence of competing DNA was measured by a restriction fragment binding assay (Figure 3). In this experiment the TFO was radiolabeled, incubated with unlabeled plasmid (pGS37) DNA fragments, and electrophoresed through an agarose gel to assess triplex formation. Of eleven different restriction fragments generated in the digests, only the two containing the intron 1 target sequence bound TFO1. A more stringent test of binding specificity was carried out using competition experiments performed with genomic DNA isolated from a Chinese hamster ovary cell line in which the native APRT gene was deleted. At a 1×10^5-fold excess of hamster genomic DNA (in base pairs), binding of TFO1 was reduced less than 10-fold (Figure 4). This result implies that the dissociation constant for specific binding is approximately 10^4-fold lower than that for nonspecific binding to genomic DNA.

Kinetics of TFO1 Binding to the Intron 1 Site. In order to examine the kinetics of triplex formation, experiments were carried out under pseudo-first-order conditions with duplex $< 10^{-10}$ M, and [TFO] = 10^{-10} to 10^{-7} M, so that the concentration of TFO changed by less than 10% over the entire time course of each reaction. Triplex reaction time courses were performed under standard conditions with radiolabeled target duplex, extents of triplex formation were quantitated and the results were analyzed by fitting the data for each [TFO] to a single-exponential function:

$$F(t) = F_\infty(1 - (\exp[-k_\psi t]))$$

where $F(t)$ is the fraction of duplex converted to triplex at time t, F_∞ is the equilibrium value determined by [TFO] and K_d, and k_ψ is the pseudo-first-order rate constant for triplex formation at a given concentration of TFO. A K_d value of 7×10^{-10} M was obtained from reactions incubated for 88 h (Figure 5A). At low concentrations (*e.g.*, 10^{-9} M, Figure 5B) triplex formation was extremely slow, with a half-life for completion of the reaction near 17 h, corresponding to a k_ψ of 1.1×10^{-5} s^{-1}. The rate constant, k_ψ, increased linearly with increasing TFO concentration, consistent with simple second-order kinetics (Figure 5C).

For a simple bimolecular model of triplex (T) formation from duplex (D) and TFO (S), S + D $\rightleftharpoons$ T, the fraction of triplex (F) formed as a function of time is determined by two rate constants. If the second-order forward rate constant for formation is k_2, and the first-order dissociation rate constant is k_1, then under pseudo-first-order conditions ($[S]_0 \sim [S]_\infty$),

$$F(t) = (k_2[S]/(k_2[S] + k_1))(1 - \exp[-[k_2[S] + k_1]t])$$

Equivalently, if the equilibrium dissociation constant is $K_d = [S][D]/[T] = k_1/k_2$, then F is given by

$$F(t) = ([S]/([S] + K_d))(1 - \exp[-(k_2([S] + K_d)t])$$

so that the time course of triplex formation should be a single-exponential function beginning at time zero and approaching the equilibrium value of $F = F_\infty = [S]/([S] + K_d)$ with a pseudo-first-order rate constant of $k_\psi = k_2([S] + K_d)$, or in logarithmic form, $\log k_\psi = \log k_2 + \log([S] + K_d)$. Thus a plot of $\log k_\psi$ *vs* $\log([S] + K_d)$ should have a unit slope and a Y intercept of k_2, and it should approach a value of $\log k_\psi = \log k_1$ as [S] approaches zero (*i.e.*, as $[S] + K_d \rightarrow K_d$). Figure 5C shows that such a plot of our kinetic results gives a best fit slope of 1.01 and a value of $k_2 = 2.3 \times 10^4$ M^{-1} s^{-1}. From the extrapolated value of k_ψ at [S] = 0, $k_1 = 1.1 \times 10^{-5}$ s^{-1}, while the value of k_1 from the simple calculation $k_1 = k_2K_d$ gives a value of 1.6×10^{-5} s^{-1}. Thus the results are consistent with simple second-order kinetics for triplex formation. In contrast to the very slow dissociation rate constant (k_1) observed in the presence of Mg^{2+}, the rapid dissociation of triplexes in gels lacking Mg^{2+} (see below) suggests that the effect of Mg^{2+} on triplex stability is largely through slowing of TFO dissociation from the triple-helical complex.

Magnesium Dependence of Triplex Formation. In order to determine the levels of magnesium required for TFO1 to bind its target duplex, a range of [$MgCl_2$] was used in gel mobility shift assays. $MgCl_2$ (10 mM) was included in the

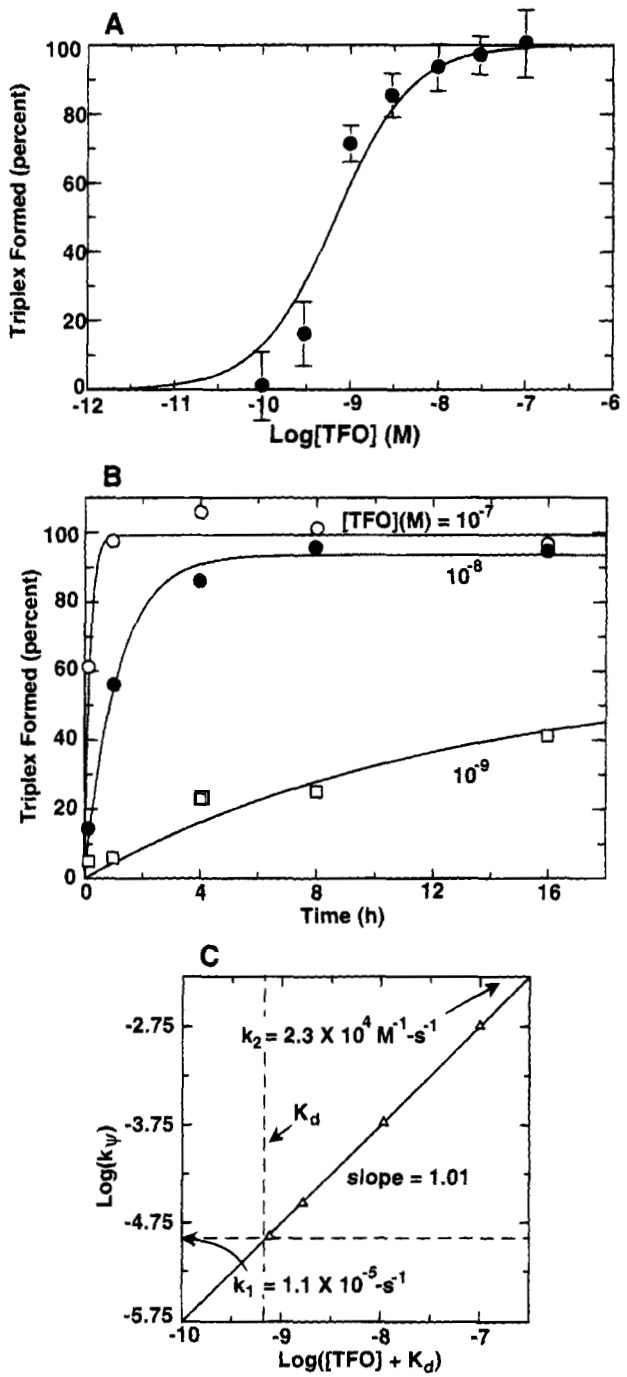

FIGURE 5: Kinetics of triplex formation. (A) Equilibrium binding. The K_d value for TFO1 binding to its target duplex was determined to be 7×10^{-10} M using least squares fitting of the data points obtained from band shift analyses. Increasing concentrations of TFO were titrated into ^{32}P-labeled duplex, and samples were incubated for 88 h at 37 °C to ensure equilibrium. The percent of triplex formed is plotted as a function of $\log_{10}$[TFO]. (B) Time course for triplex formation. Samples were incubated at 37 °C for 0−64 h under standard conditions for band shift analysis. Gels were dried, and radioactivity was quantitated. The plot shows fraction of triplex formed with time at 10^{-9}, 10^{-8}, and 10^{-7} M TFO. (C) Determination of rate constants. Pseudo-first-order rate constants (k_ψ) were determined from time courses of triplex formation, and the $\log_{10}(k_\psi)$ was plotted as a function of $\log_{10}([\text{TFO}] + K_d)$. From linear least squares fitting, slope = 1.01, $k_1 = 1.1 \times 10^{-5}$ s^{-1}, and $k_2 = 2.3 \times 10^4$ M^{-1} s^{-1}.

gels to stabilize triplexes formed prior to electrophoresis, because we found, consistent with previous results (Cooney et al., 1988; Durland et al., 1991), that in the absence of

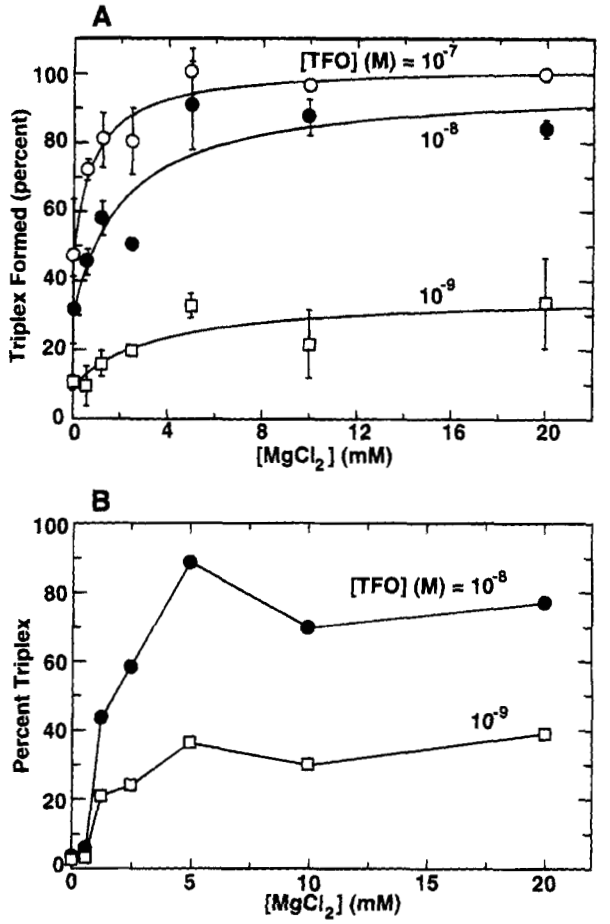

FIGURE 6: Formation of triplexes in the presence of $MgCl_2$. The formation of triplex was monitored using quantitative gel mobility shift assays after incubation in buffer (10 mM Tris-HCl, pH 7.6, 1 mM spermine, and 10% sucrose) in the presence of increasing concentrations of $MgCl_2$. Samples were analyzed by 12% PAGE, buffered in 89 mM Tris, 89 mM boric acid, and either (A) 10 mM $MgCl_2$ or (B) [$MgCl_2$], the same as in the incubation buffer. The plots show percent triplex formed as a function of [$MgCl_2$] in the reaction mixture.

Mg^{2+} triplexes rapidly dissociated during electrophoresis, regardless of the [$MgCl_2$] present in the reaction mixture. When assayed using Mg^{2+}-containing gels, triplex formation was detectable even when the TFO was incubated with target duplex in the absence of added $MgCl_2$ or other divalent cations; the extent of triplex formation after a 15-h incubation with [TFO] at either 10^{-9} or 10^{-8} M and zero added Mg^{2+} was about one-third of the maximal extent observed at higher [Mg^{2+}] (Figure 6A). The kinetics of triplex formation are sufficiently slow (see above) to rule out significant formation of triplex in the gel during electrophoresis, as was confirmed by the absence of triplex formation when duplex and TFO were mixed and then immediately subjected to electrophoresis (data not shown).

Maximal triplex formation was observed at 5 mM Mg^{2+}; increases in [Mg^{2+}] to 10 or 20 mM did not further enhance triplex formation. In order to determine the range of [$MgCl_2$] required in the gel to stabilize the triplexes during electrophoresis, a study was performed with equimolar [$MgCl_2$] in the incubation buffer and the gel system (Figure 6B). The curves in Figure 6B differ significantly from those in Figure 6A only below 1 mM Mg^{2+}, indicating that ≥ 1 mM Mg^{2+} is required in the gel to stabilize triplexes during electrophoresis.

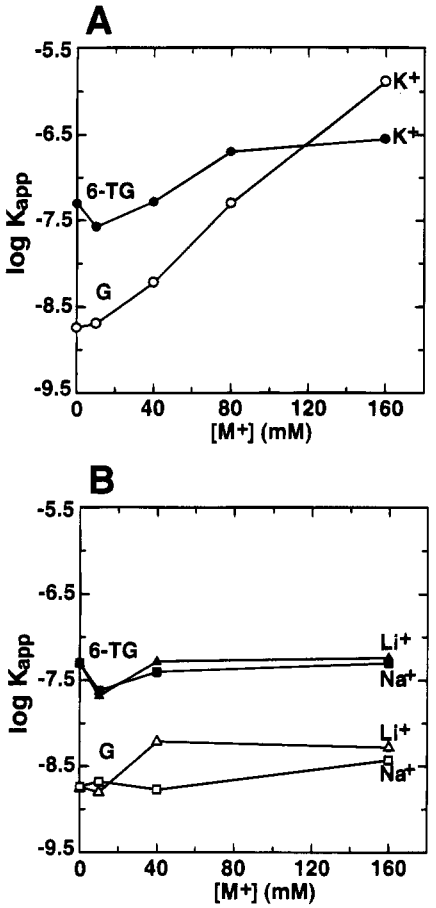

FIGURE 7: Influence of monovalent cations on triplex formation. Apparent dissociation constants (K_{app}) for TFO1 and TFO2 determined by nonlinear least squares fitting of data obtained by band shift analysis, after incubations with varying concentrations of the indicated cations. The effects of (A) KCl or (B) NaCl, and LiCl on the binding of TFO1 (G) or TFO2 (6-TG) to target duplex are shown. Solutions contained 10 mM Tris-HCl, pH 7.6, 1 mM spermine, 10 mM $MgCl_2$, 10% sucrose, and varying concentrations of the monovalent cation indicated, and were incubated at 37 °C for 15 h prior to electrophoresis.

Monovalent Cation Effects on Triplex Formation. To assess the effect of monovalent cations on triplex formation, band shift analysis was carried out after incubation of duplex and TFO under various salt conditions. At a given concentration of KCl, NaCl, or LiCl, ranging from 0 to 160 mM, increasing amounts of either TFO1 or the 6-TG modified TFO (TFO2; Table 1) were mixed with 5′-^{32}P-labeled 38-mer duplex in a standard triplex binding buffer. Reactions were incubated at 37 °C for 15 h and assessed for triplex formation. Results are shown in Figure 7.

As shown in Figure 7A, in the presence of K^+, there is a steeply cooperative concentration dependence for triplex formation with TFO1 that is not seen with the 6-TG modified TFO2. This effect is specific for K^+, as both TFO1 and TFO2 show a much weaker dependence on the presence of either Na^+ or Li^+ ions (Figure 7B). At 10 mM all of the monovalent salts had little effect on triplex formation by TFO1 or TFO2. However, as salt concentrations were increased to 40 or 160 mM, triplex formation by TFO1 was decreased, with potencies in the order $K^+ \gg Li^+ \geq Na^+$. Binding by TFO2 was slightly enhanced by all three salts at low salt concentrations, and inhibition of triplex formation only became predominant in the case of K^+, and only at concentrations of 80 and 160 mM. Even at 160 mM KCl the negative effect on triplex formation by TFO2 was ~250-fold weaker than the effect on TFO1.

DISCUSSION

Triplex Formation with High Affinity and High Specificity in a Selectable Gene. The recognition of APRT intron 1 by TFO1 represents the first example of high-affinity targeted triplex formation within a mammalian gene that is readily susceptible to both positive and negative selection in cell culture. The only comparable triplex target site currently known is the much lower affinity one in the promoter region of the dihydrofolate reductase gene (Gee et al., 1992). Our characterization of the triplex formation reaction lays the groundwork for applications within living cells. The high affinity and specificity of TFO1 binding to its target site bode well for the ability of externally applied oligonucleotides, which are efficiently transported into living cells and readily enter target nuclei (Yakubov et al., 1989), to form triplexes at relatively low intracellar concentrations. Both TFO1 and the 6-TG-substituted TFO2 should form triplex at micromolar concentrations at physiological [K^+].

Kinetics of Triplex Formation. The kinetics of triplex formation are also important for intracellular applications. We found this to be a remarkably slow process, with a rate constant on the order of 2×10^4 M^{-1} s^{-1}. This is approximately 3 orders of magnitude slower than would be expected for diffusion-limited kinetics, implying many unproductive encounters between duplex and TFO prior to triplex formation. Such slow kinetics are to be expected if productive reaction with the TFO requires the duplex to adopt a rarely sampled conformation. NMR studies of triplex DNA (Radhakrishnan & Patel, 1994) have provided evidence for a conformation of the underlying duplex intermediate between A-form and B-form DNA. The combination of slow kinetics and high-affinity binding has important implications for the intracellular persistence of triplexes, once formed. Our kinetic results also underscore the importance, when studying triplex equilibria, either of allowing sufficient time for equilibrium to be established or of determining K_d values indirectly from rate constants for formation and dissociation.

Cation Effects on Triplex Formation. The effects of cations on triplex formation are complex. In general, the screening by salts of electrostatic repulsion between duplex and TFO phosphates should give rise to a favorable contribution of cations to triplex formation, as we and others have observed for Mg^{2+} and polyamines [*e.g.*, Cooney et al. (1988) and Singleton and Dervan (1993)]. Electrostatic screening is also consistent with the slight enhancement of TFO2 binding by monovalent cations even in the presence of Mg^{2+}. However, the substantial inhibition of triplex formation by K^+, but not by Na^+ or Li^+, does not fit into this simple model of electrostatic screening. The high specificity for K^+ and the steeply cooperative concentration dependence suggest that specific binding sites and simultaneous action of multiple potassium ions are involved.

The mechanism for the inhibitory effect of potassium, which is qualitatively similar to that observed with other triplexes of the purine:purine:pyrimidine type (Cheng & Van Dyke, 1993; Milligan et al., 1993), is unclear. Physiological concentrations of KCl are capable of stabilizing the formation of tetraplexes with G-rich oligonucleotides (Williamson et al., 1989; Sen & Gilbert, 1990), so such structures may

partially explain our results and earlier observations of inhibition of triplex formation by monovalent cations (Cheng & Van Dyke, 1993; Hanvey et al., 1991). The decreased potency of K^+ in reducing triplex formation by TFO2, in which three bases have been replaced by 6-thioguanosine, is consistent with this idea. However, our observation that neither Li^+ nor Na^+ significantly suppresses triplex formation suggests that tetraplex structures (if formed) have properties that differ from those previously characterized. In addition, we have been unable to detect any higher order structures formed by TFO1 by shifts in the electrophoretic mobility of TFO1 (data not shown); in contrast, G-quartet formation has been readily observed by this technique (Williamson et al., 1989; Sen & Gilbert, 1990). In order to determine whether the negative effect on triplex formation by K^+ was due to inhibition of association, acceleration of dissociation, or both, an experiment was performed, adding KCl or NaCl at 160 mM to preformed triplex. Preliminary results showed a substantial increase in the rate of triplex dissociation with KCl, but less effect with NaCl (data not shown). This result suggests that a competing TFO self-association reaction is unlikely to account for all of the observed K^+ effect. An alternative mechanism is simple competition with Mg^{2+} or spermine for cation binding sites that are stabilized much more effectively by higher valence cations, as has been suggested for pyrimidine triplexes (Singleton & Dervan, 1993). However, there would have to be specific geometric constraints at the binding sites to account for the ineffectiveness of Na^+ and Li^+. A combination of ion competition and kinetic studies should allow these hypotheses to be tested.

Chemical Modifications of Triplex-Forming Oligonucleotides. An advantage of oligonucleotide-based strategies for gene manipulation via triplex formation is the ability to incorporate chemical modifications into the TFOs used for targeting. For example, the 3′-propanolamine modification used in our experiments has been found to increase *in vivo* stability of the TFO (Zendegui et al., 1991). In addition, various photoreactive compounds and metal chelates can be conjugated to TFOs to induce site-specific DNA damage (Moser & Dervan, 1987; Takasugi et al., 1991). The incorporation of photoinducible or other DNA-damaging agents into TFOs should facilitate studies of the effects of site-specific DNA damage on recombination and mutation.

Because of the absence of favorably situated hydrogen bond donors and acceptors, the T:C-G base triplet formed in the intron 1 site at position 564, where TFO1 contains a T, is not expected to contribute favorably to triplex formation, and may contribute unfavorably. Several T analogs have been tested for triplex formation, and 5FU was found to enhance binding in the range of 10−60-fold, depending on the number of Ts replaced (Durland et al., 1994). The present study tested two modifications that might be expected to alleviate this unfavorable effect: (1) substitution of T by 5FU to enhance the H-bonding potential by addition of the electron-withdrawing group; and (2) an imidazole-type substitution, to alleviate the potential steric hindrance of thymine's N3 proton and cytosine's C4 amino proton. These modified bases did not significantly enhance triplex formation at the intron 1 site. Thus, the detailed structure at these sites within the triplexes formed by all three TFOs probably differs from what current models (Radhakrishnan & Patel, 1994) would predict and remains to be determined. Such structural information will be important for designing TFO modifications that can overcome the negative contributions of a pyrimidine base within the purine-rich strand of a target duplex.

It is perhaps somewhat less surprising that substitution in the TFO of 6-thioguanosine for G, which provides much of the driving force for triplex formation through G:G-C triplets, lowers the affinity of the TFO binding its target duplex. This substitution also significantly lowers triplex sensitivity to K^+, presumably through a weaker interaction of sulfur than of oxygen with K^+ (Gee et al., 1995; see discussion of cation effects above).

Prospects for Triplex Targeting within the APRT Gene. The triple-helical complex formed by TFO1 and the APRT intron 1 site appears to have many of the characteristics necessary for addressing the effects of triplex formation and triplex-directed DNA damage on recombination, mutation, and gene expression: high affinity, high specificity, a long bound lifetime, and a convenient location in a gene in which rare molecular events can be readily detected. Striking effects on gene transcription, mutation, and replication have been observed with triplexes that form with much lower affinity (Postel et al., 1991; McShan et al., 1992; Grigoriev et al., 1993; Ing et al., 1993; Havre & Glazer, 1993; Havre et al., 1993; Birg et al., 1990). Further modifications of TFO1 may allow even more efficient and precise manipulation of the APRT gene. Intercalating agents or other groups conferring additional duplex binding affinity may allow higher efficiency triplex formation at physiological $[K^+]$. Furthermore, attachment of photoreactive groups to TFO1 could allow introduction of damaged sites in the APRT gene with high efficiency and precise temporal control. Preliminary results indicate that triplex formation at the intron 1 site can occur with a variety of photosensitizing agents attached to the 3′ end of TFO1. Thus, further modifications of TFO1 and observation of their effects on triplex formation represent interesting areas for future studies.

ACKNOWLEDGMENT

We thank Robert Tinder for the synthesis of the oligonucleotides.

REFERENCES

Adair, G. M., Nairn, R. S., Wilson, J. H., Scheerer, J. B., & Brotherman, K. A. (1990) *Somatic Cell Mol. Genet. 16*, 437−441.

Beal, P. A., & Dervan, P. B. (1991) *Science 251*, 1360−1363.

Birg, F., Praseuth, D., Zerial, A., Thuong, N. T., Asseline, U., LeDoan, T., & Helene, C. (1990) *Nucleic Acids Res. 18*, 2901−2908.

Bond, J. P., Anderson, C. F., & Record, T. M., Jr. (1994) *Biophys. J. 67*, 825−836.

Botstein, D., & Fink, G. (1988) *Science 240*, 1439−1443.

Capecchi, M. R. (1989) *Science 244*, 1288−1292.

Cheng, A. J., & Van Dyke, M. W. (1993) *Nucleic Acids Res. 21*, 5630−5635.

Cooney, M., Czernuszewicz, G., Postel, E. H., Flint, S. J., & Hogan, M. E. (1988) *Science 241*, 456−459.

Durland, R. H., Kessler, D. J., Gunnel, S., Duvic, M., Pettitt, B. M., & Hogan, M. E. (1991) *Biochemistry 30*, 9246−9255.

Durland, R. H., Rao, T. S., Revankar, G. R., Tinsley, J. H., Myrick, M. A., Seth, D. M., Rayford, J., Singh, P., & Jayaraman, K. (1994) *Nucleic Acids Res. 22*, 3233−3240.

Duval-Valentin, G., Thuong, N. T., & Helene, C. (1992) *Proc. Natl. Acad. Sci. U.S.A. 89*, 504−508.

Felsenfeld, G., Davies, D. R., & Rich, A. (1957) *J. Am. Chem. Soc. 79*, 2023−2024.

Gee, J. E., Blume, S., Snyder, R. C., Ray, R., & Miller, D. M. (1992) *J. Biol. Chem. 267*, 11163−11167.
Gee, J. E., Revankar, G. R., Rao, T. S., & Hogan, M. E. (1995) *Biochemistry* (in press).
Grigoriev, M., Praseuth, D., Robin, P., Hemar, A., Saison-Behmoaras, T., Dautry-Varsat, A., Thuong, N. T., Helene, C., & Harel-Bellan, A. (1992) *J. Biol. Chem. 267*, 3389−3395.
Grigoriev, M., Praseuth, D., Guieysse, A. L., Robin, P., Thuong, N. T., Helene, C., & Harel-Bellan, A. (1993) *Proc. Natl. Acad. Sci. U.S.A. 90*, 3501−3505.
Hanvey, J. C., Williams, E. M., & Besterman, J. M. (1991) *Antisense Res. Dev. 1*, 307−317.
Havre, P. A., & Glazer, P. M. (1993) *J. Virol. 67*, 7324−7331.
Havre, P. A., Gunther, E. J., Gasparro, F. P., & Glazer, P. M. (1993) *Proc. Natl. Acad. Sci. U.S.A. 90*, 7879−7883.
Ing, N. H., Beekman, J. M., Kessler, D. J., Murphy, M., Jayaraman, K., Zendegui, J. G., Hogan, M. E., O'Malley, B. W., & Tsai, M. (1993) *Nucleic Acids Res. 21*, 2789−2796.
Ito, T., Smith, C. L., & Cantor, C. R. (1992) *Proc. Natl. Acad. Sci. U.S.A. 89*, 495−498.
Jetter, M. C., & Hobbs, F. W. (1993) *Biochemistry 32*, 3249−3254.
Kessler, D. J., Pettitt, B. M., Cheng, Y., Smith, S. R., Jayaraman, K., Vu, H. M., & Hogan, M. E. (1993) *Nucleic Acids Res. 21*, 4810−4815.
Krawczyk, S. H., Milligan, J. F., Wadwani, S., Moulds, C., Froehler, B. C., & Matteucci, M. D. (1992) *Proc. Natl. Acad. Sci. U.S.A. 89*, 3761−3764.
Le Doan, T., Perrouault, L., Asseline, U., Thuong, N. T., Rivalle, C., Bisagni, E., & Helene, C. (1991) *Antisense Res. Dev. 1*, 43−54.
Maher, L. J., III, Wold, B., & Dervan, P. B. (1989) *Science 245*, 725−730.
Maher, J. L., III, Dervan, P. B., & Wold, B. J. (1990) *Biochemistry 29*, 8820−8826.
Mansour, S. L., Thomas, K. R., & Capecchi, M. R. (1988) *Nature 336*, 348−352.
Mayfield, C., Squibb, M., & Miller, D. (1994) *Biochemistry 33*, 3358−3363.
McShan, W. M., Rossen, R. D., Laughter, A. H., Trial, J., Kessler, D. J., Zendegui, J. G., Hogan, M. E., & Orson, F. M. (1992) *J. Biol. Chem. 267*, 5712−5721.
Milligan, J. F., Krawczyk, S. H., Wadwani, S., & Matteucci, M. D. (1993) *Nucleic Acids Res. 21*, 327−333.
Moser, H. E., & Dervan, P. B. (1987) *Science 238*, 645−650.
Pei, D., Corey, D. R., & Schultz, P. G. (1990) *Proc. Natl. Acad. Sci. U.S.A. 87*, 9858−9862.
Pennington, S. L., & Wilson, J. H. (1991) *Proc. Natl. Acad. Sci. U.S.A. 88*, 9498−9502.
Perrouault, L., Asseline, U., Rivalle, C., Thuong, N. T., Bisagni, E., Giovannangeli, C., Le Doan, T., & Helene, C. (1990) *Nature 344*, 358−360.
Pilch, D. S., Levenson, C., & Shafer, R. H. (1991) *Biochemistry 30*, 6081−6088.
Postel, E. H., Flint, S. J., Kessler, D. J., & Hogan, M. E. (1991) *Proc. Natl. Acad. Sci. U.S.A. 88*, 8227−8231.
Povsic, T. J., & Dervan, P. B. (1989) *J. Am. Chem. Soc. 111*, 3059−3061.
Radhakrishnan, I., & Patel, D. J. (1994) *Biochemistry 33*, 11405−11416.
Rajagopal, P., & Feigon, J. (1989) *Nature 339*, 637−640.
Rao, T. S., Jayaraman, K., Durland, R. H., & Revenkar, G. R. (1992) *Tetrahedron Lett. 33*, 7651−7654.
Rothstein, R. (1983) *Methods Enzymol. 101*, 202−211.
Rougee, M., Faucon, B., Mergny, J. L., Barcelo, F., Giovannangeli, C., Garestier, T., & Helene, C. (1992) *Biochemistry 31*, 9269−9278.
Sen, D., & Gilbert, W. (1990) *Nature 344*, 410−414.
Shindo, H., Torigoe, H., & Sarai, A. (1993) *Biochemistry 32*, 8963−8969.
Singleton, S. F., & Dervan, P. B. (1992) *Biochemistry 31*, 10995−11003.
Singleton, S. F., & Dervan, P. B. (1993) *Biochemistry 32*, 13171−13179.
Stilz, H. U., & Dervan, P. B. (1993) *Biochemistry 32*, 2177−2185.
Strobel, S. A., & Dervan, P. B. (1991) *Nature 350*, 172−174.
Takasugi, M., Guendouz, A., Chassignol, M., Decout, J. L., Lhomme, J., Thuong, N. T., & Helene, C. (1991) *Proc. Natl. Acad. Sci. U.S.A. 88*, 5602−5606.
Thomas, T., & Thomas, T. J. (1993) *Biochemistry 32*, 14068−14074.
Thuong, N. T., & Helene, C. (1993) *Angew. Chem., Int. Ed. Engl. 32*, 666−690.
Vu, H., Singh, P., Joyce, N., Hogan, M. E., & Jayaraman, K. (1993) *Nucleic Acids Symp. Ser. 29*, 19.
Williamson, J. R., Raghuraman, M. K., & Cech, T. R. (1989) *Cell 59*, 871−880.
Yakubov, L. A., Deeva, E. A., Zarytova, V. F., Ivanova, E. M., Ryte, A. S., Yurchenko, L. V., & Vlassov, V. V. (1989) *Proc. Natl. Acad. Sci. U.S.A. 86*, 6454−6458.
Zendegui, J. G., Vasquez, K. M., Tinsley, J. H., Kessler, D. J., & Hogan, M. E. (1992) *Nucleic Acids Res. 20*, 307−314.

BI950203D